Membrane curvature directs the localization of Cdc42p to novel foci required for cell–cell fusion

Jean A. Smith,[1]* Allison E. Hall,[1]* and Mark D. Rose[1,2]

[1]Department of Molecular Biology, Princeton University, Princeton, NJ
[2]Department of Biology, Georgetown University, Washington, DC

Cell fusion is ubiquitous in eukaryotic fertilization and development. The highly conserved Rho–GTPase Cdc42p promotes yeast fusion through interaction with Fus2p, a pheromone-induced amphiphysin-like protein. We show that in prezygotes, Cdc42p forms a novel Fus2p-dependent focus at the center of the zone of cell fusion (ZCF) and remains associated with remnant cell walls after initial fusion. At the ZCF and during fusion, Cdc42p and Fus2p colocalized. In contrast, in shmoos, both proteins were near the cortex but spatially separate. Cdc42p focus formation depends on ZCF membrane curvature: mutant analysis showed that Cdc42p localization is negatively affected by shmoo-like positive ZCF curvature, consistent with the flattening of the ZCF during fusion. BAR-domain proteins such as the fusion proteins Fus2p and Rvs161p are known to recognize membrane curvature. We find that mutations that disrupt binding of the Fus2p/Rvs161p heterodimer to membranes affect Cdc42p ZCF localization. We propose that Fus2p localizes Cdc42p to the flat ZCF to promote cell wall degradation.

Introduction

During sexual reproduction, the combination of haploid gamete genomes requires fusion (Gadella and Evans, 2011; Shinn-Thomas and Mohler, 2011). In multicellular organisms, cell fusion is also required for muscle, vertebrate eye, and placenta development (Shi et al., 2009; Huppertz and Gauster, 2011; Shinn-Thomas and Mohler, 2011; Kim et al., 2015). Cell fusion has also recently been implicated in cancer development and progression (Parris, 2013; Bastida-Ruiz et al., 2016). Despite the significance of cell fusion, relatively little is known about the molecular mechanisms and regulation.

Cell fusion occurs during mating of the budding yeast *Saccharomyces cerevisiae* to form a diploid zygote. Haploid yeast cells of mating types **a** and α secrete pheromones that are detected by the other mating type. The pheromone response results in induction of mating-specific genes, cell-cycle arrest, and polarized growth (Merlini et al., 2013; Alvaro and Thorner, 2016). Altered morphogenesis results in pear-shaped cells known as "shmoos." After the shmoo tips come into contact, the cell walls and membranes flatten out, forming a synapse-like region called the zone of cell fusion (ZCF). The ZCF marks the site where the cell wall will be removed and the plasma membranes fuse (Gammie et al., 1998; Ydenberg and Rose, 2008; Merlini et al., 2013).

Several genes have been identified that are thought to be direct regulators of cell fusion. *FUS1*, *FUS2*, and *PRM1* are expressed only after pheromone induction (Trueheart et al., 1987; Elion et al., 1995; Heiman and Walter, 2000). Kel1p, a kelch protein, and Rvs161p, an amphiphysin, promote fusion but have alternative roles in regulating mitotic exit and endocytosis, respectively (Crouzet et al., 1991; Brizzio et al., 1998; Philips and Herskowitz, 1998; Höfken and Schiebel, 2002; Seshan et al., 2002; Knaus et al., 2005; Friesen et al., 2006; Smith and Rose, 2016). Fus1p is a heavily glycosylated type I membrane protein thought to act as a scaffold for cell fusion proteins (Trueheart et al., 1987; Trueheart and Fink, 1989). Fus2p is a BAR-domain protein (Stein et al., 2015) that is initially sequestered in the nucleus but then enters the cytoplasm after cell-cycle arrest (Ydenberg and Rose, 2009; Kim and Rose, 2012) where it interacts with Rvs161p (Brizzio et al., 1998; Stein et al., 2015). The heterodimer is transported to the shmoo tip dependent on actin and Myo2p (Paterson et al., 2008; Sheltzer and Rose, 2009), where it is anchored at the cortex dependent upon Fus1p, actin, and Kel1p (Paterson et al., 2008; Smith and Rose, 2016). Mutations in *FUS1*, *FUS2*, *RVS161*, and *KEL1* block the removal of the cell wall between the mating cells (Trueheart et al., 1987; Trueheart and Fink, 1989; Gammie et al., 1998; Smith and Rose, 2016). Prm1p is a transmembrane protein that promotes plasma membrane fusion after cell wall removal (Heiman and Walter, 2000).

Cdc42p is a highly conserved essential Rho-like GTPase with several roles during growth and morphogenesis, in-

*J.A. Smith and A.E. Hall contributed equally to this paper.

Correspondence to Mark D. Rose: mark.rose@georgetown.edu

J.A. Smith's present address is Dept. of Biology, The University of North Carolina at Chapel Hill, Chapel Hill, NC.

Abbreviation used: ZCF, zone of cell fusion.

The Rockefeller University Press
J. Cell Biol. Vol. 216 No. 12 3971–3980
https://doi.org/10.1083/jcb.201703169

cluding establishment of polarity, reorganization of the actin cytoskeleton, polarized secretion, budding, and activation of p21-activated kinases (Madden and Snyder, 1998; Johnson, 1999; Richman et al., 1999; Kozminski et al., 2000; Adamo et al., 2001; Perez and Rincón, 2010). During yeast mating, Cdc42p functions in three pathways: pheromone signaling (Simon et al., 1995; Zhao et al., 1995), morphogenesis (Nern and Arkowitz, 1998, 1999), and cell fusion (Barale et al., 2006; Ydenberg et al., 2012). Although the functions of Cdc42p early in the mating pathway (signaling and morphogenesis) are understood, the function of Cdc42p in cell fusion has remained unclear. Cdc42p interacts with Fus2p, and cell fusion–specific alleles of *cdc42* defective for Fus2p binding exhibit a cell fusion defect (Ydenberg et al., 2012), without having a significant effect on signaling or morphogenesis. Fus2p preferentially binds GTP-bound Cdc42p, suggesting that it recruits activated Cdc42p (Nelson et al., 2004; Ydenberg et al., 2012).

Proteins homologous to yeast Cdc42p are implicated in *Drosophila melanogaster*, mouse, and zebrafish myoblast fusion, mostly by promoting actin polymerization and cell polarization (Vasyutina et al., 2009; Abmayr and Pavlath, 2012). In the fission yeast *Schizosaccharomyces pombe*, early in cell fusion, active Cdc42p forms dynamic zones that explore the periphery of the cell and are required for pheromone secretion, polarization, and signaling before cell pairing (Bendezú and Martin, 2013; Merlini et al., 2016). However, little is known about cell wall degradation and plasma membrane fusion in fission yeast or whether Cdc42p plays a specific role in these later steps.

In budding yeast, mating-specific vesicles cluster at the ZCF, dependent on Fus1p and cell polarization proteins (e.g., Spa2p), and remain closely associated with the remnant cell walls after fusion (Baba et al., 1989; Gammie et al., 1998). Exocytosis is thought to release hydrolases into the periplasmic space between the cells, breaking down the cell wall to allow plasma membrane fusion. In support, active secretion is required for fusion (Grote, 2010), and deletion of two putative glucanase genes, *SCW4* and *SCW10*, causes a synthetic mating defect (Cappellaro et al., 1998).

We hypothesize that Fus2p functions in cell fusion to localize active Cdc42p to the center of the ZCF to promote cell wall degradation. However, because Cdc42p has multiple functions, it is already broadly localized at the shmoo tip (Ziman et al., 1993), raising the question of how localization could play a specific function in cell fusion. We find that Cdc42p forms a novel focus at the center of the ZCF that is required for fusion. The focus is dependent upon Fus2p and other known fusion proteins for formation and sensitive to the curvature of the ZCF. Because of the conservation of Cdc42p throughout eukaryotes and its roles in mouse and *Drosophila* myoblast fusion, these results have broad implications about the regulation of cell fusion.

Results and discussion

Cdc42p forms a focus at the center of the ZCF

On the basis of the requirement of the $Cdc42p^{GTP}$–Fus2p interaction for fusion, it was hypothesized that Fus2p localizes Cdc42p to the shmoo tip/ZCF to promote fusion (Ydenberg et al., 2012; Smith and Rose, 2016). However, Cdc42p was already known to localize to regions of active growth, like the shmoo tip, obscuring the need for specific localization during cell fusion. We therefore examined Cdc42p localization in prezygotes, using an integrating plasmid containing *CDC42* N-terminally tagged with 3xGFP (Dyer et al., 2013). Prezygotes are mating pairs that have not initiated cell wall removal. Because the tagged version is partially functional, a WT copy of *CDC42* remains at the endogenous locus.

In crosses to WT, GFP–Cdc42p–positive cells showed a discrete focus forming at the center of the ZCF (Fig. 1 A and Video 1). In the lower prezygote, GFP–Cdc42p was initially distributed across the ZCF but became tightly localized between the 3- and 6-min time points. Cell fusion occurred between the 9- and 12-min time points, after which Cdc42–GFP was more broadly localized. The upper prezygote shows a similar pattern but further along in cell fusion.

Because of the fleeting nature of the ZCF, we used a compromised (*fus1*Δ*fus2*Δ) mating partner to slow fusion to provide sufficient prezygotes for analysis. Chemical fixation of the prezygotes allowed acquisition of image stacks; deconvolution and optical slicing provided a clearer image of the ZCF. When crosses of *GFP–CDC42* × *fus1*Δ*fus2*Δ were analyzed, Cdc42p formed a bright focus at the center of the ZCF, similar to what was observed in the live-cell imaging (Fig. 1 B). In zygotes after fusion had begun, Cdc42p was concentrated at the edges of the remnant cell walls (Fig. 1 B). To quantify localization, we measured fluorescence intensity along a line through the ZCF (as denoted by the arrows in Fig. 1 B) and plotted this as a function of the distance (Fig. 1 C). A representative individual prezygote showed a strong plateau of fluorescence intensity, roughly 1 µm wide, in the center of the ZCF, five- to sixfold brighter than the surrounding cortex. This region corresponds to the initial site of cell wall degradation previously observed by electron microscopy (Gammie et al., 1998). The partially fused zygote showed two peaks corresponding to the edges of the remnant cell walls. To determine if the localization in prezygotes was simply due to polarized growth, we examined localization of GFP–Cdc42p in shmoos. Cdc42p localized broadly over the shmoo tip but was not significantly brighter in the center of the shmoo tip (Fig. 1 D), as confirmed by quantification of fluorescence intensity (Fig. 1 E). Therefore, we have identified a novel localization for Cdc42p, specific to prezygotes, at the center of the ZCF.

To quantify focus formation for a population of WT prezygotes, we measured fluorescence intensity as a function of distance across the ZCF for >120 prezygotes. The mean full width at half maximum of the focus in the WT prezygotes was 0.84 ± 0.02 µm. In shmoos and mutant cells, the distribution of Cdc42p was too irregular to allow measurement of a full width at half maximum. Instead, to compare the mean intensity and localization of Cdc42p among different strains, we normalized differences in ZCF width and variable levels of GFP among individual prezygotes. The ZCFs were set to the same width, using cubic interpolation to provide equal numbers of measurements, and the GFP intensities are reported as the ratios to the mean values of the two edges (12% on each side). After normalization, prezygotes with a Cdc42p focus showed a strong central peak of fluorescence (Fig. 1 F). The peak was broader than for a single prezygote, because of heterogeneity in the width of the ZCF. In Fig. 1 F, the error bars indicate SEM. For clarity, error bars are suppressed in later figures.

Cdc42p and Fus2p colocalize in prezygotes

Fus2p localizes to the center of the ZCF and forms an expanding ring as the remnant cell walls are degraded (Paterson et al.,

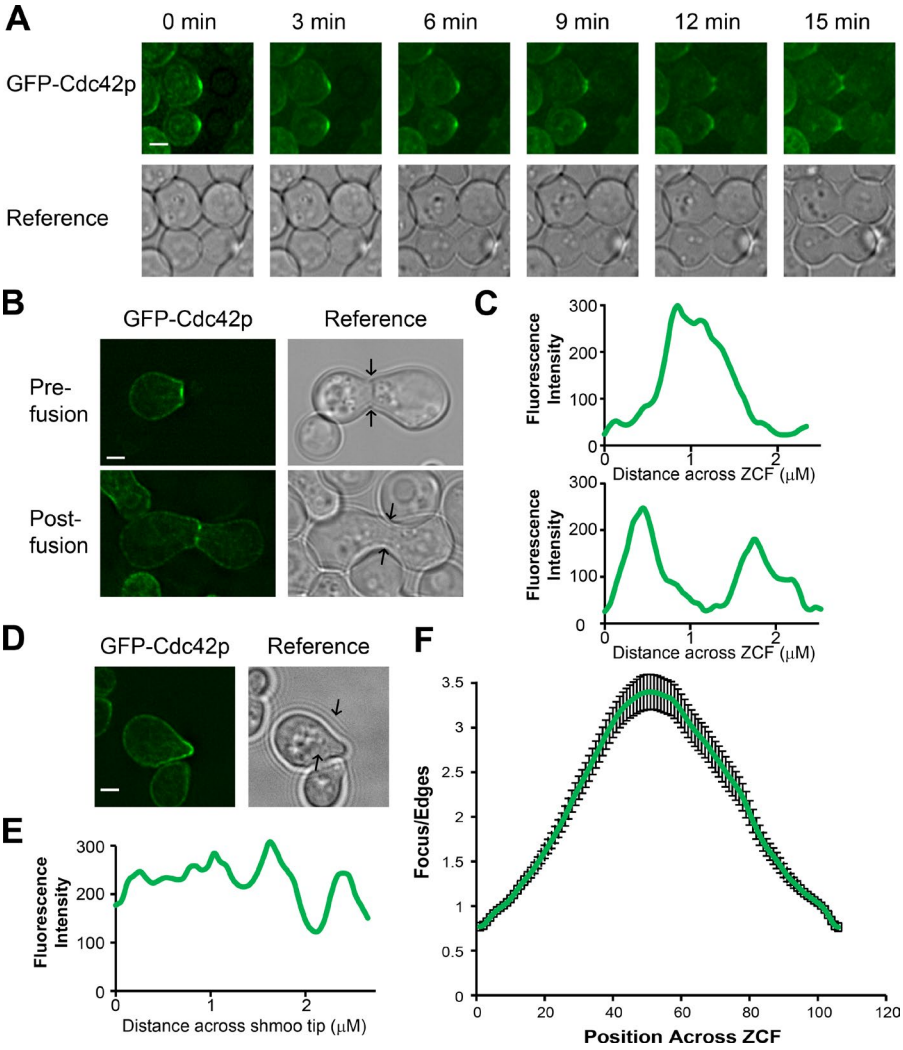

Figure 1. **Cdc42p forms a focus at the center of the ZCF.** (A) Live imaging of GFP–Cdc42p during mating. *GFP–Cdc42* cells (MY15747) were mated to WT (MY8093) and imaged at 3-min intervals. Bar, 2 µm. (B and C) Images and quantification of a representative prezygote and zygote containing GFP–Cdc42p. (B) *GFP–CDC42* cells (MY15747) were mated to a *fus1*Δ*fus2*Δ strain (JY429) for 2.5 h at 30°, fixed with 2% formaldehyde, and imaged. Bar, 2 µm. (C) The fluorescence intensity was measured from the top to the bottom of the ZCF, as denoted by the arrows on the reference image, and plotted as a function of the distance across the ZCF. (D and E) Cdc42p focus is not observed in shmoos. (D) *GFP–CDC42* cells (MY15747) were imaged after incubation with pheromone for 1.5 h. Bar, 2 µm. (E) The fluorescence intensity was measured around the shmoo tip from the top arrow to the bottom arrow, as denoted on the reference image, and plotted as a function of the distance. (F) Quantification of WT Cdc42p ZCF localization for all prezygotes imaged. Fluorescence intensities across the ZCF were measured for all prezygotes, interpolated to account for differences in ZCF length, and plotted as a ratio of the center values to the mean of the two edges. Data in F were pooled from three independent experiments. Error bars denote the SEM of all cells imaged. $n > 120$ prezygotes.

2008). Given the similarity of the Cdc42p focus to Fus2p localization, and their physical interaction, we examined their colocalization. To visualize GFP–Cdc42p and Fus2p in the same cell, we used a Fus2p construct tagged with mCherry at residue 104, where the functional Fus2p–GFP construct is tagged. Fluorescence microscopy of prezygotes showed colocalization of GFP–Cdc42p and Fus2p–mCherry at the center of the ZCF, which persisted on the remnant cell walls in postfusion zygotes (Fig. 2 A). When shmoos were imaged, colocalization was considerably more variable: some shmoos showed clear separation between the markers (Fig. 2 B, top), but partial colocalization was observed in others (Fig. 2 B, bottom). To quantify colocalization, we determined the peaks of fluorescence for GFP and mCherry along an axis orthogonal to the shmoo tip/ZCF and measured the distance between them. In prezygotes, the mean distance between the peaks was <1 pixel (1 pixel = 0.0648 µm); the distance in shmoos was almost threefold greater ($P = 0.0001$; Fig. 2 C). Therefore, Fus2p and Cdc42p colocalization is specific to prezygotes.

Cdc42p focus formation is dependent upon Fus2p and other cell fusion proteins

Colocalization of Cdc42p and Fus2p at the ZCF could be independent, perhaps because it is a specialized location, or dependent, if one protein recruits the other. Imaging of Cdc42p in a *fus2*Δ strain showed Cdc42p localized broadly across the ZCF, rather than to a central focus (Fig. 3 A). Quantification of Cdc42p localization across all *fus2*Δ prezygotes showed a significantly flatter curve than WT (Fig. 3 B; $P = 2 \times 10^{-5}$). On the basis of this analysis (Fig. 3 B), Cdc42p focus formation is dependent upon Fus2p. Mutation of Kel1p also caused a localization defect for Cdc42p (Fig. S1). As Kel1p is a known interaction partner for Fus2p (Smith and Rose, 2016), these data support our model of Fus2p regulating Cdc42p localization.

Fus1p, a pheromone-induced transmembrane protein (Trueheart et al., 1987; Trueheart and Fink, 1989), has multiple roles in cell fusion, including stabilizing Fus2p localization at the cortex (Paterson et al., 2008; Smith and Rose, 2016). Imaging of Cdc42p in a *fus1*Δ strain showed broad Cdc42p localization (Fig. 3 A) significantly flatter than WT (Fig. 3 B). Fus1p and Fus2p play partially independent roles in cell wall degradation; a synthetic mating defect is seen in double-mutant strains (Gammie et al., 1998). To determine if Fus1p affects Cdc42p localization to the ZCF entirely through Fus2p localization, we analyzed a *fus1*Δ*fus2*Δ strain. Cdc42p was even more poorly localized at the ZCF in this strain (Fig. 3, A and B). When the phenotype was quantified, Cdc42p localization in *fus1*Δ*fus2*Δ was significantly worse than either *fus1*Δ ($P = 0.008$) or *fus2*Δ ($P = 0.0001$). Because Fus1p itself is localized broadly across the shmoo tip (Trueheart et al., 1987; Nelson et al., 2004;

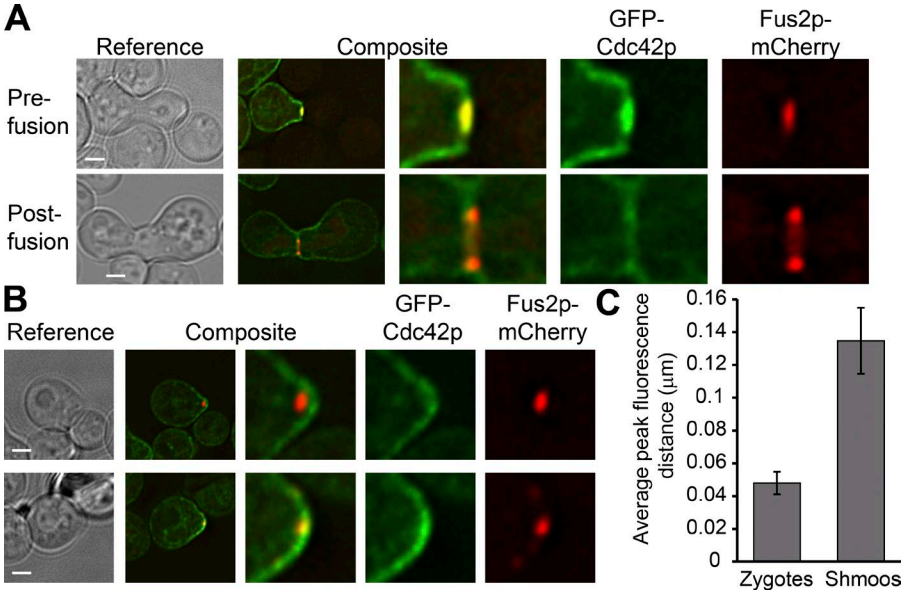

Figure 2. **Cdc42p and Fus2p colocalize specifically at the ZCF.** (A) Cdc42p and Fus2p colocalize at the ZCF and at the remnant cell walls. *GFP–CDC42 fus2*Δ cells containing Fus2p–mCherry$_{104}$ on a plasmid (pMR5821) were mated to a *fus1*Δ*fus2*Δ strain (JY429) for 2.5 h at 30°, fixed with 2% formaldehyde, and imaged. (B) Cdc42p and Fus2p do not colocalize in shmoos. The same *MAT***a** strain as in A was imaged after incubation with pheromone for 1.5 h. (C) Quantification of the distance between GFP and mCherry fluorescence peaks for both prezygotes and shmoos. *n* = 50 prezygotes or shmoos imaged. Error bars denote the SEM. Data in C were pooled from three independent experiments. Bars, 2 µm.

Barfield et al., 2009), we hypothesize that Fus2p is the main regulator of Cdc42p focus formation, whereas Fus1p plays an additional minor role in Cdc42p localization (Fig. 3 B).

To confirm that the phenotypic difference between the mutants is specific to the ZCF, we analyzed Cdc42p localization in WT, *fus1*Δ, *fus2*Δ, and *fus1*Δ*fus2*Δ shmoos. As expected, Cdc42p localized broadly across the shmoo tip in all of these strains, with no obvious focus at the shmoo tip (Fig. 3 C). Quantification showed only a modest peak at the shmoo tip (Fig. 3 D), rather than the large peak seen at the ZCF (Fig. 3 B), consistent with the lack of a focus in shmoos. There was no significant difference between WT versus *fus1*Δ (P = 0.3) or *fus1*Δ*fus2*Δ (P = 0.5). Deletion of *FUS2* caused a slight reduction relative to WT (P = 0.015), which was not significantly different from either *fus1*Δ (P = 0.4) or *fus1*Δ*fus2*Δ (P = 0.4). We therefore conclude that both Fus1p and Fus2p are required for Cdc42p focus formation at the ZCF and that the localization of Cdc42p in shmoos is largely independent of both proteins.

The *cdc42–138* allele (D122A), in the rho-insert domain, eliminates the interaction between Cdc42p and Fus2p and causes a cell fusion defect (Ydenberg et al., 2012). When the *cdc42–138* mutation was introduced into GFP-tagged *CDC42*, GFP–Cdc42p^{138} localized broadly over the ZCF, similar to the *fus1*Δ*fus2*Δ phenotype (Fig. 3, E and F). Previous evidence showed that the cortical localization of Fus2p was not affected by *cdc42–138* in shmoos (Ydenberg et al., 2012). However, because the ZCF behaves differently from the shmoo tip, we examined localization of Fus2p in *cdc42–138* prezygotes. GFP-tagged Fus2p localized to the center of the ZCF in *cdc42–138* prezygotes, with a fluorescence intensity of 70% of Fus2p in WT prezygotes (Fig. 3, G and H). We conclude that loss of the Cdc42p–Fus2p interaction does not have a large effect on Fus2p localization but greatly affects Cdc42p localization to the ZCF. The determinants for Fus2p localization are not altered by the *cdc42–138* mutation, but reduced Cdc42p interaction may affect the stability of Fus2p at the ZCF.

The ZCF is distinct from the shmoo tip

The behavior of Cdc42p suggests that there are important physiological and/or regulatory differences between the ZCF and the shmoo tip. Fus2p/Rvs161p localization to the shmoo tip also differs in its requirements relative to the ZCF. First, mutations affecting polarization (*spa2*, *bni1*) have a major effect on shmoo-tip localization but only a minor effect on ZCF localization (Paterson et al., 2008). Second, although the C terminus of Fus2p is essential for shmoo-tip localization, a truncated protein, Fus2p$^{1–650}$, localizes to the ZCF with almost WT morphology and efficiency (Fig. S2). Thus localization of Fus2p/Rvs161p to the shmoo-tip cortex requires additional interactions. These observations indicate that the shmoo tip is a poor proxy for the ZCF and suggests that Fus2p/Rvs161p localized at the shmoo tip is not competent for recruiting Cdc42p.

Cdc42p localizes to flat interfaces

Given that Fus1p and Fus2p are both expressed and localized to the shmoo tip, but are not required for Cdc42p localization in shmoos, the question arises as to what is different in prezygotes that leads to focus formation at the ZCF. Although there are several possibilities, we note that one prominent difference between the shmoo tip and the ZCF is the curvature of the plasma membrane. As cells polarize toward each other and shmoo, an area of strong positive curvature is formed (Fig. 4 A). However, after cells come into contact and grow together, the cell walls and plasma membranes flatten, reducing the previous positive curvature at the shmoo tip to zero (Fig. 4 A). Given that the BAR-domain proteins, which include Fus2p/Rvs161p, are known to recognize membrane curvature (Rao and Haucke, 2011), we hypothesized that the change in curvature may comprise a key signal for Cdc42p focus formation. To test this hypothesis, we sought to identify conditions in which the ZCF in prezygotes would have positive, negative, or zero curvature.

Deletion of *FPS1*, which encodes a glycerol efflux pump, causes increased cellular osmotic pressure and a cell fusion defect (Philips and Herskowitz, 1997). However, unlike all other fusion proteins in which deletion of the gene in both mating partners exacerbates the defect, deletion of *FPS1* in both mating partners actually suppresses the cell fusion defect. The authors suggested that imbalanced osmotic pressure between two mating partners might signal to stop cell fusion. We hypothesized that the imbalanced osmotic pressure might be manifest by changes in the curvature at the ZCF. To determine this, we analyzed crosses of *FPS1* or *fps1*Δ mated to either *fus1*Δ*fus2*Δ or *fus1*Δ-

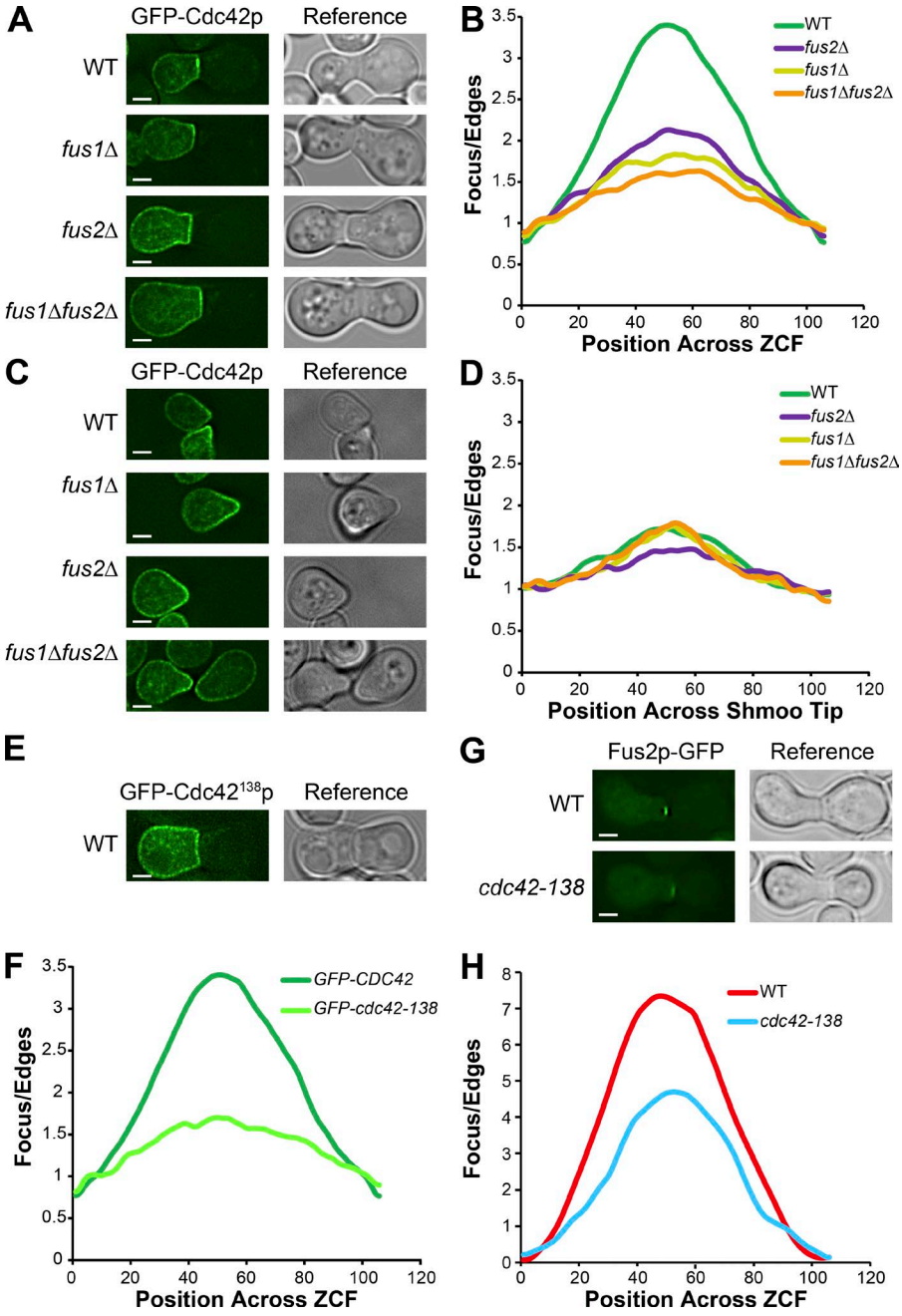

Figure 3. **Cdc42p focus formation is dependent on both Fus1p and Fus2p.** (A and B) Deletion of *FUS1* or *FUS2* cause defects in Cdc42p focus formation. (A) Representative images of prezygotes. WT (MY15747), *fus1*Δ (MY15752), *fus2*Δ (MY15717), and *fus1*Δ*fus2*Δ (MY15748) strains all containing *GFP–CDC42* were mated to a *fus1*Δ*fus2*Δ strain (JY429) for 2.5 h at 30°, fixed with 2% formaldehyde, and imaged. (B) Quantification of Cdc42p ZCF localization for all prezygotes imaged. Fluorescence intensities across the ZCF were measured for all prezygotes, interpolated to account for differences in ZCF length, and plotted as a ratio of the center values to the mean of the two edges. $n \geq 75$ prezygotes per strain. (C and D) Cdc42p localization in shmoos is independent of Fus1p and Fus2p. (C) Representative images of shmoos. The same strains as in A were imaged after treatment with pheromone for 1.5 h. (D) Quantification of the fluorescence across the shmoo tip for all shmoos imaged. Fluorescence intensities were measured across the shmoo tip for all shmoos, interpolated, and plotted as a ratio of the center values to the mean of the two edges. $n \geq 37$ shmoos per strain. (E and F) Cdc42p^{138} does not form a ZCF focus. (E) Representative images of GFP–Cdc42p^{138} prezygotes. *GFP–cdc42–138* (MY15789) was mated to a *fus1*Δ*fus2*Δ strain (JY429) for 2.5 h at 30°, fixed with 2% formaldehyde, and imaged. (F) Quantification of Cdc42p^{138} ZCF localization in prezygotes. $n \geq 84$ prezygotes per strain. (G and H) Fus2p localization to the ZCF is not strongly altered in *cdc42–138*. (G) Representative images of Fus2p–GFP in WT (MY15588) and Cdc42p^{138} (MY15590) cells, both mated to *fus1*Δ*fus2*Δ (JY429). (H) Quantification of Fus2p across the ZCF in prezygotes. Fluorescence intensities across the ZCF were measured for all prezygotes, interpolated to account for differences in ZCF length, and plotted as a ratio of the center values to the mean of the two edges. $n \geq 22$ for each strain. Bars, 2 µm.

*fus2*Δ*fps1*Δ. We used *fus1*Δ*fus2*Δ to allow imaging of the ZCF, because *fps1*Δ × *fps1*Δ zygotes do not have a fusion defect, and the ZCF is therefore fleeting. When mating partners were imaged with a membrane-specific lipophilic dye, FM4-64, the ZCF appeared curved if either partner lacked *FPS1* (Fig. 4 B). However, curvature of the ZCF was suppressed when both mating partners lacked *FPS1*, consistent with the hypothesis that imbalanced osmotic pressure causes the *fps1*Δ cell to bulge into its partner. To quantify the curvature of the ZCF, we measured the radius of a circle whose chord matches the interface. A flat ZCF matches a very large circle and so has a large radius, whereas a highly curved ZCF matches a small circle with a small radius. When this measurement was performed on the GFP-containing cells, the mean radius of ZCF curvature was more than 4 times smaller for the *fps1*Δ parent mated to *FPS1*, relative to the *FPS1* × *FPS1* or *fps1*Δ × *fps1*Δ prezygotes (Fig. 4 C).

To determine if ZCF curvature affects Cdc42p localization, we imaged GFP–Cdc42p in the same crosses. Cdc42p was partially mislocalized when the partner containing GFP–Cdc42p had positive curvature, as in the *GFP–CDC42 fps1*Δ × *FPS1* mating (Fig. 4, D and E). This phenotype was significantly worse than WT (P = 0.001) However, mislocalization in the *fps1*Δ strain was completely suppressed when the same strain was mated to an *fps1*Δ strain (Fig. 4 D, compare bottom panels); Cdc42p localization in this case was indistinguishable from WT (P = 0.2). Cdc42p localization was only affected by positive curvature; the *GFP–CDC42* × *fps1*Δ mating, in which the GFP-positive cell has a negatively curved ZCF, exhibited WT Cdc42p localization. When the mating orientation was switched such that the GFP-positive cell was *MAT*α, the same results were obtained, showing that the fusion defect and suppression are not mating type specific (Fig. 4 F). Given

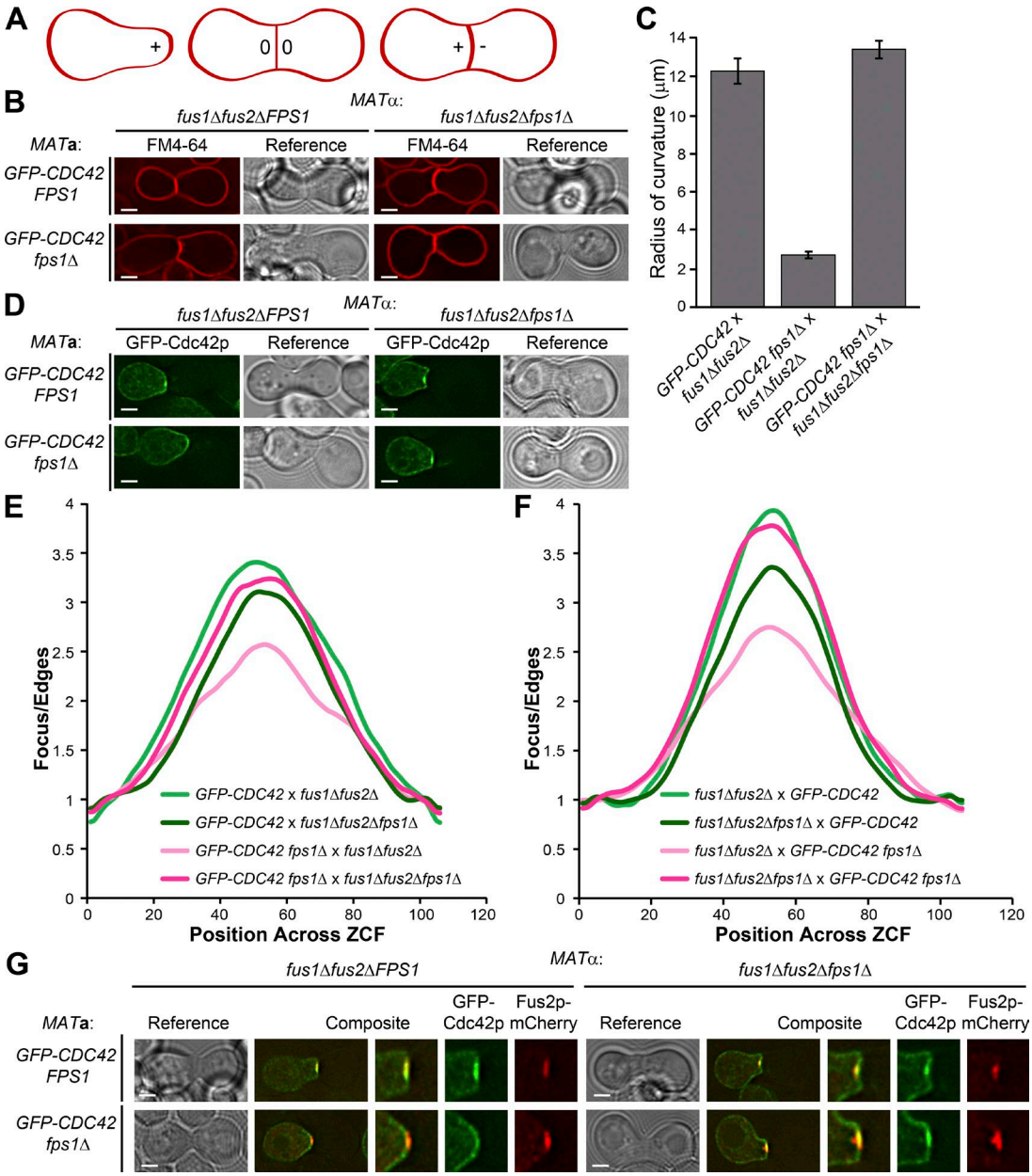

Figure 4. **Cdc42p localizes to flat interfaces.** (A) Model of curvature in shmoos, WT prezygotes, or curved prezygotes. (B and C) Deletion of *FPS1* in one mating partner causes a curved ZCF. (B) Representative images of FM4-64-stained prezygoes. *GFP–CDC42* (MY15747) and *GFP–CDC42 fps1*Δ (MY15864) cells were mated against either a *fus1*Δ*fus2*Δ (JY429) or *fus1*Δ*fus2*Δ*fps1*Δ strain (MY15877) for 2.5 h at 30°, resuspended in TAF buffer, stained with FM4-64, and imaged. (C) Quantification of the radius of curvature in *fps1*Δ strains. The radius of the largest circle whose chord matches the contour of the ZCF of the GFP-positive cell was measured and averaged across all cells imaged. $n \geq 56$ prezygotes per strain, from two or more experiments. Error bars denote the SEM. (D–F) Cdc42p is mislocalized in mating partners with a positively curved ZCF. (D) Representative images of prezygotes. The same matings were performed as in B for 2.5 h at 30°, fixed with 2% formaldehyde, and imaged. (E and F) Quantification of Cdc42p ZCF localization. Crosses are listed as *MAT*a x *MAT*α. $n \geq 89$ prezygotes per strain. (G) Positively curved ZCFs do not alter Fus2p localization. *GFP–CDC42* (MY15747) and *GFP–CDC42 fps1*Δ (MY15864) cells were transformed with *FUS2–mCherry*$_{104}$ (pMR5821), mated against either a *fus1*Δ*fus2*Δ (JY429) or *fus1*Δ*fus2*Δ*fps1*Δ strain (MY15877) for 2.5 h at 30°, fixed with 2% formaldehyde, and imaged. Bars, 2 µm.

that Cdc42p mislocalization in the *fps1*Δ strain is suppressed by differences in the osmotic pressure of its partner, we conclude that Cdc42p localization is not directly regulated by the osmolarity of the cell.

Could Cdc42p localization in the *fps1*Δ strain be indirectly regulated by altered pheromone signaling? As for osmotic regulation, if deletion of *FPS1* affected cell fusion via pheromone signaling, then *fps1*Δ × *fps1*Δ matings should exacerbate the cell fusion defect rather than suppress it. The finding that Cdc42p is mislocalized in *fps1*Δ × *FPS1* matings but does form a focus in *fps1*Δ × *fps1*Δ matings argues that signaling defects cannot account for the difference. We conclude that the most likely difference between the shmoo tip and the ZCF is the curvature of the plasma membrane.

Because Cdc42p localization is dependent on Fus2p localization, we examined Fus2p in the same mating partners. We found that Fus2p–mCherry was localized to the ZCF in all four matings (≥94% of all prezygotes; Fig. 4 G). Given that

Fus2p was localized in all cases, even when Cdc42p was not, we conclude that curvature specifically affects the interaction between Fus2p and Cdc42p.

A role for the Fus2p/Rvs161p membrane-binding domain in Cdc42p ZCF localization

How might curvature affect the interaction between Fus2p/Rvs161p and Cdc42p? BAR domain–containing proteins have been identified as membrane curvature sensing and generating proteins for many cellular processes (Zimmerberg and Kozlov, 2006; Suetsugu et al., 2014; McMahon et al., 2015). BAR domains comprise dimers of helix bundles (Qualmann et al., 2011). Electrostatic interactions with positively charged surface residues mediate initial binding (McMahon et al., 2015). Modeling of Fus2p/Rvs161p revealed two regions that would be strongly positively charged: the concave inner surface and the lateral outer surface (Stein et al., 2015). Previous work showed that mutations of conserved lysine residues in Fus2p and Rvs161p caused mating defects but did not disrupt binding to each other, suggesting that they affect other functions (Stein et al., 2015). The "con" mutations reside on the concave surface of the predicted banana-shaped heterodimer, and the "loop" mutations reside at the tips of the heterodimer (Stein et al., 2015). Although most of these mutations are expected to disrupt localization to the membrane, others might affect the conformation of Fus2p/Rvs161p at the membrane. An initial screen of localization in shmoos (Table S3) identified one allele, *fus2*^{con}, that caused a strong defect in mating (Stein et al., 2015) but retained close to WT localization (76%). We hypothesized that this mutation might alter the conformation of Fus2p/Rvs161p at the ZCF, compromising its ability to recruit Cdc42p. Fus2p^{con} was localized to the ZCF in 81% of *fus2*^{con} prezygotes (Fig. 5 A). Another mutant with a comparable mating defect, *rvs161*^{loop}, exhibited only 14% Fus2p localization (Fig. 5 A). In both the *fus2*^{con} and *rvs161*^{loop} mutants, Cdc42p was broadly distributed along the ZCF, similar to *fus2*Δ (Fig. 5, A and B). These data suggest that the mating defect in the *fus2*^{con} mutant is due to the failure of Fus2p to recruit Cdc42p to the ZCF.

These data combine to produce a model in which Fus2p/Rvs161p localize to the curved shmoo tip in polarizing cells, with the complex in an orientation in which it does not interact with Cdc42p. As prezygote formation occurs, the change from positive to zero curvature would cause Fus2p/Rvs161p to undergo a conformational change, allowing interaction with Cdc42p.

The BAR protein superfamily comprises multiple subfamilies that adopt conformations with a variety of intrinsic curvatures. BAR domains are 16–23 nm in length (Qualmann et al., 2011), implying that they should be sensitive to curvature at the nanometer scale (Zimmerberg and Kozlov, 2006). However, the Cdc42p focus is much larger, 1 µm in diameter. Recently, it was found that fungal septins can distinguish micrometer-scale curvature; single septin complexes bind preferentially to micrometer-scale curved membranes and are stabilized by polymerization (Bridges et al., 2016). BAR domains also oligomerize, forming filamentous polymers in vitro (McMahon et al., 2015; Suetsugu, 2016). Possibly, like septins, polymerization of BAR-domain proteins would allow membrane curvature sensing over many tens or hundreds of nanometers.

Flattening of the ZCF membrane may facilitate Fus2p/Rvs161p polymerization, perhaps relying on electrostatic interactions between the concave face of one dimer and the convex face of the other (Stein et al., 2015). Polymerization may

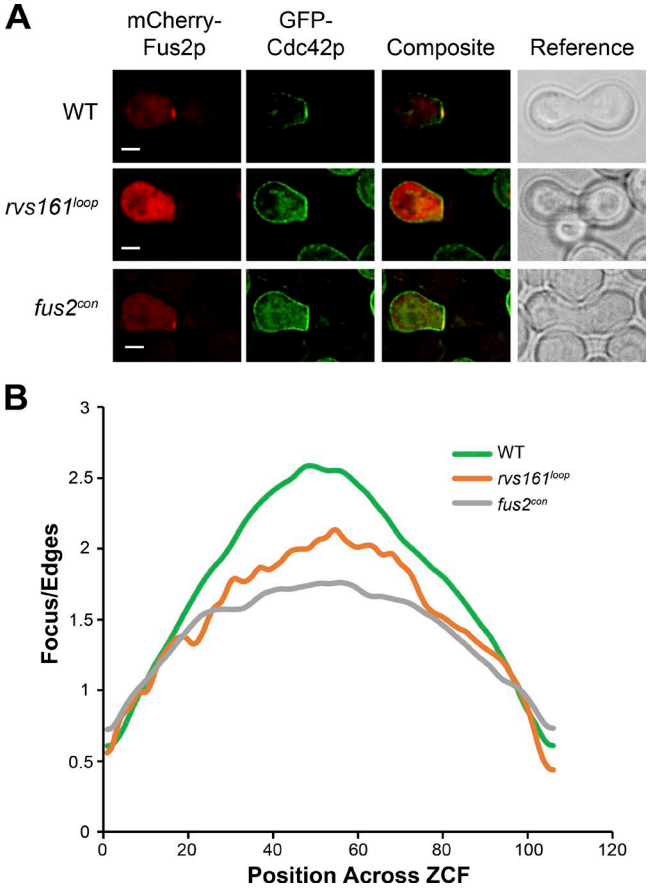

Figure 5. **Lysine residue mutations in the Fus2p/Rvs161p amphiphysin-like dimer affect Cdc42p ZCF localization.** (A) Representative images of prezygotes. *GFP–CDC42 fus2*Δ *rvs161*Δ (MY16013) cells were transformed with both a *FUS2–mCherry*$_{104}$ plasmid (pMR5821) and a Rvs161p–Flag$_{85}$ (pMR7155) or Rvs161p–Flag$_{85}$ and mCherry–*fus2*^{con} (pMR7158) or *FUS2–mCherry*$_{104}$ and GFP–*rvs161*^{loop} (pMR7157) and mated against a *fus1*Δ*fus2*Δ (JY429) for 2.5 h at 30°, fixed with 2% formaldehyde, and imaged. (B) Quantification of Cdc42p ZCF localization. Fluorescence intensities across the ZCF were measured for all prezygotes, interpolated to account for differences in ZCF length, and plotted as a ratio of the center values to the mean of the two edges. Data were pooled from three independent experiments. $n \geq 54$ for each strain. Bars, 2 µm.

induce a conformation change in Fus2p/Rvs161p, promoting Cdc42p binding and focus formation. As cell fusion continues, the Fus2p/Rvs161p/Cdc42p complex remains associated with the edge of the remnant cell walls, even as free Fus2p returns to the nucleus (Paterson et al., 2008; Ydenberg and Rose, 2009). The edge of the remnant cell wall has strong negative curvature, a natural fit for the concave face of the dimer. After the remnant cell walls are removed, the cortex of the zygote is once again smooth with overall positive curvature.

Because yeast live in hypoosmotic conditions, cell wall removal during mating must be tightly regulated. During growth, cell wall damage is quickly sensed and repaired, as shown by the rapid localization of Pkc1p to sites of laser damage (Kono et al., 2012). Therefore, yeast cells must distinguish between removal at the shmoo tip, where degradation would be fatal, and at the ZCF. Recently, it was suggested that cell wall degradation at the ZCF is driven solely by the contact-dependent increase in the concentration of cell wall remodeling enzymes due to reduced diffusion at the ZCF (Huberman and Murray, 2014). Multiple lines of evidence suggest this is not sufficient for cell

fusion. First, several mutations block cell fusion without affecting prezygote formation or general cell wall remodeling processes (e.g., *fus1*Δ and *fus2*Δ). Second, the behavior of *fps1*Δ suggests that cell fusion is regulated. Finally, the localization of Cdc42p suggests that cells use curvature to distinguish whether they have formed a prezygote. Sensing sites of zero or negative curvature may be a general mechanism of regulation. BAR-domain proteins have roles in hemagglutinin-promoted cell–cell fusion (Richard et al., 2011) and mouse myoblast fusion (Ho et al., 2004; Simionescu-Bankston et al., 2013; George et al., 2014; Kim et al., 2015). Therefore, curvature sensing may be a conserved mechanism in regulating and/or promoting cell fusion.

Materials and methods

General yeast techniques

Yeast media, general methods, and transformations were performed as described previously (Amberg et al., 2005), with minor modifications. Cells were grown in yeast extract peptone dextrose or selective media to maintain plasmids. Transformations were performed by growing cells to log phase (OD_{600} 0.4–0.6), washing once with water, and resuspending in transformation mixture (33% wt/vol polyethylene glycol 4000, 0.1 M Li-acetate, and 0.2 mg/ml single-stranded carrier DNA), together with 1 µg plasmid DNA or 10 µl of a PCR in a final volume of 360 µl. Strains and plasmids are listed in Tables S1 and S2. All strains and plasmids are available upon request. Deletion strains were created either via PCR amplification of selective markers and homologous recombination at the locus of interest or via sporulation and tetrad dissection. GFP-Cdc42p was provided by D. Lew (Duke University, Durham, NC). Mutations in pMR5821 were created via PCR-mediated site-directed mutagenesis. All strains were grown at 30°C. For pheromone induction experiments, early exponential cells growing in selective media were treated for 90 min with synthetic α-factor (Department of Molecular Biology Syn/Seq Facility, Princeton University) added to a final concentration of 10 µg/ml.

Yeast mating assays

Quantitative filter-matings were performed as described previously, with minor alterations (Gammie and Rose, 2002), by mixing early exponential *MAT***a** cells with *MAT*α cells in a 1:4 ratio to reach a total of 10^7 cells/ml. This ratio was determined to be optimal for mating efficiency of the *MAT***a** cells, while showing the lowest variance. The cells were mixed together, concentrated on 25-mm, 0.45-µm nitrocellulose filter disks (Millipore Corporation), and incubated on rich media plates for 2.5–3 h at 30°C.

Microscopy

For imaging of pheromone-induced cells with fluorescent proteins, cells were induced by addition of 10 µg/ml α-factor for 90 min, fixed for 10 min with 2% formaldehyde at 30°C, washed in 1× PBS, and then imaged in PBS. All images except those in Fig. 3 (G and H) and Fig. 5 were acquired at 23°C using a deconvolution microscopy system (DeltaVision; Applied Precision, LLC) equipped with an inverted microscope (TE200; Nikon), a 100× objective with numerical aperture of 1.4, and a CoolSnap HQ2 Camera (Photometrics). Deconvolution and image analysis were performed using softWoRx and ImageJ (National Institutes of Health). Data for Fig. 3 (G and H) and Fig. 5 were acquired at 23°C using a TI-E inverted microscope (Nikon) equipped with a 100× objective with numerical aperture of 1.45 and an Orca Flash4 camera. NIS Elements (Nikon) software was used for image acquisition along with NIS Elements automatic 3D deconvolution and ImageJ for analysis.

For imaging of prezygotes containing fluorescent proteins, mating mixtures were prepared as described in the previous section on yeast mating assays, resuspended in synthetic media, fixed for 10 min with 2% formaldehyde at 30°C, and imaged as above. Quantification of fluorescence was performed using ImageJ software (Schindelin et al., 2012, 2015). Values along the ZCF were interpolated using cubic interpolation in MATLAB (The MathWorks). The Mann-Whitney test for two independent samples was used to obtain p-values for localization curves unless otherwise stated. Quantification of colocalization of Cdc42p and Fus2p was performed by quantifying fluorescence across a line perpendicular to the shmoo tip or ZCF using ImageJ software. Fus2p and Cdc42p intensities were determined by measuring fluorescence intensity at the ZCF using an elliptical region of interest in ImageJ and normalized to fluorescence intensity at the opposite end of the cell. Error bars represent the SEM for all cells imaged. A two-tailed, two-sample unequal *t* test was used to determine significance.

Microscopic assays of FM4-64-stained mating mixtures were performed as described previously (Grote, 2008). Mating mixtures were prepared as described in the previous section on yeast mating assays, and then resuspended in 1 ml TAF buffer (20 mM Tris-HCl, 20 mM NaN_3, and 20 mM NaF in water) and kept on ice. FM4-64 (Molecular Probes/Invitrogen) was added to mating mixtures to a final concentration of 4 µM, and stained zygotes were imaged as described in the first paragraph of this section.

Live imaging was performed by mixing 0.02 OD_{600} of each mating type and allowing cells to mate on a 2% agarose pad at 23°C. Images were taken at 3-min intervals using the DeltaVision system described in the first paragraph under Microscopy.

Online supplemental material

Video 1 shows live imaging of GFP–Cdc42p during cell fusion of WT mating pairs. Cdc42p forms a focus just before cell fusion. Fig. S1 shows that deletion of Kel1p, a fusion protein known to interact with Fus2p, disrupts Cdc42p localization to the ZCF. Fig. S2 shows that removal of the C terminus of Fus2p does not disrupt its localization to the ZCF. Yeast strains and plasmids used are listed in Tables S1 and S2, respectively. Table S3 reports the mating efficiency and localization of Fus2p–GFP in mutants affecting the Fus2p/Rvs161p BAR domain.

Acknowledgments

We thank members of the Rose and Gammie laboratories for helpful support and discussion. We thank Corey Ashby for developing the MATLAB tool for cubic interpolation of fluorescence data. We especially thank Danny Lew for providing the GFP-tagged *CDC42*. We also thank Zemer Gitai for the use of his microscope.

This work was supported by National Institutes of Health grant GM037739 (to M.D. Rose). J.A. Smith and A.E. Hall were supported by National Institutes of Health training grant GM007388.

The authors declare no competing financial interests.

Author contributions: J.A. Smith and A.E. Hall conceived, conducted, and analyzed experiments. M.D. Rose conceived, analyzed, and supervised experiments. All three authors took part in writing, reviewing, and editing the manuscript.

Submitted: 23 March 2017
Revised: 8 September 2017
Accepted: 22 September 2017

References

Abmayr, S.M., and G.K. Pavlath. 2012. Myoblast fusion: lessons from flies and mice. *Development.* 139:641–656. https://doi.org/10.1242/dev.068353

Adamo, J.E., J.J. Moskow, A.S. Gladfelter, D. Viterbo, D.J. Lew, and P.J. Brennwald. 2001. Yeast Cdc42 functions at a late step in exocytosis, specifically during polarized growth of the emerging bud. *J. Cell Biol.* 155:581–592. https://doi.org/10.1083/jcb.200106065

Alvaro, C.G., and J. Thorner. 2016. Heterotrimeric G protein-coupled receptor signaling in yeast mating pheromone response. *J. Biol. Chem.* 291:7788–7795. https://doi.org/10.1074/jbc.R116.714980

Amberg, D.C., D.J. Burke, and J.N. Strathem. 2005. Methods in Yeast Genetics: A Cold Spring Harbor Laboratory Course Manual. Cold Spring Harbor Laboratory Press, Cold Spring Harbor, NY.

Baba, M., N. Baba, Y. Ohsumi, K. Kanaya, and M. Osumi. 1989. Three-dimensional analysis of morphogenesis induced by mating pheromone alpha factor in *Saccharomyces cerevisiae*. *J. Cell Sci.* 94:207–216.

Barale, S., D. McCusker, R.A. Arkowitz, and D. Nice. 2006. Cdc42p GDP/GTP cycling is necessary for efficient cell fusion during yeast mating. *Mol. Biol. Cell.* 17:2824–2838. https://doi.org/10.1091/mbc.E05-11-1040

Barfield, R.M., J.C. Fromme, and R. Schekman. 2009. The exomer coat complex transports Fus1p to the plasma membrane via a novel plasma membrane sorting signal in yeast. *Mol. Biol. Cell.* 20:4985–4996. https://doi.org/10.1091/mbc.E09-04-0324

Bastida-Ruiz, D., K. Van Hoesen, and M. Cohen. 2016. The dark side of cell fusion. *Int. J. Mol. Sci.* 17:E638. https://doi.org/10.3390/ijms17050638

Bendezú, F.O., and S.G. Martin. 2013. Cdc42 explores the cell periphery for mate selection in fission yeast. *Curr. Biol.* 23:42–47. https://doi.org/10.1016/j.cub.2012.10.042

Bridges, A.A., M.S. Jentzsch, P.W. Oakes, P. Occhipinti, and A.S. Gladfelter. 2016. Micron-scale plasma membrane curvature is recognized by the septin cytoskeleton. *J. Cell Biol.* 213:23–32. https://doi.org/10.1083/jcb.201512029

Brizzio, V., A.E. Gammie, and M.D. Rose. 1998. Rvs161p interacts with Fus2p to promote cell fusion in *Saccharomyces cerevisiae*. *J. Cell Biol.* 141:567–584. https://doi.org/10.1083/jcb.141.3.567

Cappellaro, C., V. Mrsa, and W. Tanner. 1998. New potential cell wall glucanases of *Saccharomyces cerevisiae* and their involvement in mating. *J. Bacteriol.* 180:5030–5037.

Crouzet, M., M. Urdaci, L. Dulau, and M. Aigle. 1991. Yeast mutant affected for viability upon nutrient starvation: characterization and cloning of the RVS161 gene. *Yeast.* 7:727–743. https://doi.org/10.1002/yea.320070708

Dyer, J.M., N.S. Savage, M. Jin, T.R. Zyla, T.C. Elston, and D.J. Lew. 2013. Tracking shallow chemical gradients by actin-driven wandering of the polarization site. *Curr. Biol.* 23:32–41. https://doi.org/10.1016/j.cub.2012.11.014

Elion, E.A., J. Trueheart, and G.R. Fink. 1995. Fus2 localizes near the site of cell fusion and is required for both cell fusion and nuclear alignment during zygote formation. *J. Cell Biol.* 130:1283–1296. https://doi.org/10.1083/jcb.130.6.1283

Friesen, H., C. Humphries, Y. Ho, O. Schub, K. Colwill, and B. Andrews. 2006. Characterization of the yeast amphiphysins Rvs161p and Rvs167p reveals roles for the Rvs heterodimer in vivo. *Mol. Biol. Cell.* 17:1306–1321. https://doi.org/10.1091/mbc.E05-06-0476

Gadella, B.M., and J.P. Evans. 2011. Membrane fusions during mammalian fertilization. *In* Cell Fusion in Health and Disease. T. Dittmar, and K.S. Zänker, editors. Springer Netherlands, Dordrecht. 65–80. https://doi.org/10.1007/978-94-007-0763-4_5

Gammie, A.E., and M.D. Rose. 2002. Assays of cell and nuclear fusion. Methods Enzymol. 351:477–498.

Gammie, A.E., V. Brizzio, and M.D. Rose. 1998. Distinct morphological phenotypes of cell fusion mutants. *Mol. Biol. Cell.* 9:1395–1410. https://doi.org/10.1091/mbc.9.6.1395

George, B., N. Jain, P. Fen Chong, J. Hou Tan, and T. Thanabalu. 2014. Myogenesis defect due to Toca-1 knockdown can be suppressed by expression of N-WASP. *Biochim. Biophys. Acta.* 1843:1930–1941. https://doi.org/10.1016/j.bbamcr.2014.05.008

Grote, E. 2008. Cell fusion assays for yeast mating pairs. *Methods Mol. Biol.* 475:165–196.

Grote, E. 2010. Secretion is required for late events in the cell-fusion pathway of mating yeast. *J. Cell Sci.* 123:1902–1912. https://doi.org/10.1242/jcs.066662

Heiman, M.G., and P. Walter. 2000. Prm1p, a pheromone-regulated multispanning membrane protein, facilitates plasma membrane fusion during yeast mating. *J. Cell Biol.* 151:719–730. https://doi.org/10.1083/jcb.151.3.719

Ho, H.Y.H., R. Rohatgi, A.M. Lebensohn, J. Le Ma, J. Li, S.P. Gygi, and M.W. Kirschner. 2004. Toca-1 mediates Cdc42-dependent actin nucleation by activating the N-WASP-WIP complex. *Cell.* 118:203–216. https://doi.org/10.1016/j.cell.2004.06.027

Höfken, T., and E. Schiebel. 2002. A role for cell polarity proteins in mitotic exit. *EMBO J.* 21:4851–4862. https://doi.org/10.1093/emboj/cdf481

Huberman, L.B., and A.W. Murray. 2014. A model for cell wall dissolution in mating yeast cells: polarized secretion and restricted diffusion of cell wall remodeling enzymes induces local dissolution. *PLoS One.* 9:e109780. https://doi.org/10.1371/journal.pone.0109780

Huppertz, B., and M. Gauster. 2011. Trophoblast fusion. *Adv. Exp. Med. Biol.* 713:81–95. https://doi.org/10.1007/978-94-007-0763-4_6

Johnson, D.I. 1999. Cdc42: an essential Rho-type GTPase controlling eukaryotic cell polarity. *Microbiol. Mol. Biol. Rev.* 63:54–105.

Kim, J., and M.D. Rose. 2012. A mechanism for the coordination of proliferation and differentiation by spatial regulation of Fus2p in budding yeast. *Genes Dev.* 26:1110–1121. https://doi.org/10.1101/gad.187260.112

Kim, J.H., P. Jin, R. Duan, and E.H. Chen. 2015. Mechanisms of myoblast fusion during muscle development. *Curr. Opin. Genet. Dev.* 32:162–170. https://doi.org/10.1016/j.gde.2015.03.006

Knaus, M., E. Cameroni, I. Pedruzzi, K. Tatchell, C. De Virgilio, and M. Peter. 2005. The Bud14p-Glc7p complex functions as a cortical regulator of dynein in budding yeast. *EMBO J.* 24:3000–3011. https://doi.org/10.1038/sj.emboj.7600783

Kono, K., Y. Saeki, S. Yoshida, K. Tanaka, and D. Pellman. 2012. Proteasomal degradation resolves competition between cell polarization and cellular wound healing. *Cell.* 150:151–164. https://doi.org/10.1016/j.cell.2012.05.030

Kozminski, K.G., A.J. Chen, A.A. Rodal, and D.G. Drubin. 2000. Functions and functional domains of the GTPase Cdc42p. *Mol. Biol. Cell.* 11:339–354. https://doi.org/10.1091/mbc.11.1.339

Madden, K., and M. Snyder. 1998. Cell polarity and morphogenesis in budding yeast. *Annu. Rev. Microbiol.* 52:687–744. https://doi.org/10.1146/annurev.micro.52.1.687

McMahon, H.T., E. Boucrot, S. Aimon, A. Callan-Jones, A. Berthaud, M. Pinot, G.E. Toombes, P. Bassereau, J. Bigay, B. Antonny, et al. 2015. Membrane curvature at a glance. *J. Cell Sci.* 128:1065–1070. https://doi.org/10.1242/jcs.114454

Merlini, L., O. Dudin, and S.G. Martin. 2013. Mate and fuse: how yeast cells do it. *Open Biol.* 3:130008. https://doi.org/10.1098/rsob.130008

Merlini, L., B. Khalili, F.O. Bendezú, D. Hurwitz, V. Vincenzetti, D. Vavylonis, and S.G. Martin. 2016. Local pheromone release from dynamic polarity sites underlies cell-cell pairing during yeast mating. *Curr. Biol.* 26:1117–1125. https://doi.org/10.1016/j.cub.2016.02.064

Nelson, B., A.B. Parsons, M. Evangelista, K. Schaefer, K. Kennedy, S. Ritchie, T.L. Petryshen, and C. Boone. 2004. Fus1p interacts with components of the Hog1p mitogen-activated protein kinase and Cdc42p morphogenesis signaling pathways to control cell fusion during yeast mating. *Genetics.* 166:67–77. https://doi.org/10.1534/genetics.166.1.67

Nern, A., and R.A. Arkowitz. 1998. A GTP-exchange factor required for cell orientation. *Nature.* 391:195–198. https://doi.org/10.1038/34458

Nern, A., and R.A. Arkowitz. 1999. A Cdc24p-Far1p-Gβγ protein complex required for yeast orientation during mating. *J. Cell Biol.* 144:1187–1202. https://doi.org/10.1083/jcb.144.6.1187

Parris, G.E. 2013. Historical perspective of cell-cell fusion in cancer initiation and progression. *Crit. Rev. Oncog.* 18:1–18. https://doi.org/10.1615/CritRevOncog.v18.i1-2.20

Paterson, J.M., C.A. Ydenberg, and M.D. Rose. 2008. Dynamic localization of yeast Fus2p to an expanding ring at the cell fusion junction during mating. *J. Cell Biol.* 181:697–709. https://doi.org/10.1083/jcb.200801101

Perez, P., and S.A. Rincón. 2010. Rho GTPases: regulation of cell polarity and growth in yeasts. *Biochem. J.* 426:243–253. https://doi.org/10.1042/BJ20091823

Philips, J., and I. Herskowitz. 1997. Osmotic balance regulates cell fusion during mating in *Saccharomyces cerevisiae*. *J. Cell Biol.* 138:961–974. https://doi.org/10.1083/jcb.138.5.961

Philips, J., and I. Herskowitz. 1998. Identification of Kel1p, a kelch domain-containing protein involved in cell fusion and morphology in *Saccharomyces cerevisiae*. *J. Cell Biol.* 143:375–389. https://doi.org/10.1083/jcb.143.2.375

Qualmann, B., D. Koch, and M.M. Kessels. 2011. Let's go bananas: revisiting the endocytic BAR code. *EMBO J.* 30:3501–3515. https://doi.org/10.1038/emboj.2011.266

Rao, Y., and V. Haucke. 2011. Membrane shaping by the Bin/amphiphysin/Rvs (BAR) domain protein superfamily. *Cell. Mol. Life Sci.* 68:3983–3993. https://doi.org/10.1007/s00018-011-0768-5

Richard, J.P., E. Leikina, R. Langen, W.M. Henne, M. Popova, T. Balla, H.T. McMahon, M.M. Kozlov, and L.V. Chernomordik. 2011. Intracellular curvature-generating proteins in cell-to-cell fusion. *Biochem. J.* 440:185–193. https://doi.org/10.1042/BJ20111243

Richman, T.J., M.M. Sawyer, and D.I. Johnson. 1999. The Cdc42p GTPase is involved in a G2/M morphogenetic checkpoint regulating the apical-isotropic switch and nuclear division in yeast. *J. Biol. Chem.* 274:16861–16870. https://doi.org/10.1074/jbc.274.24.16861

Schindelin, J., I. Arganda-Carreras, E. Frise, V. Kaynig, M. Longair, T. Pietzsch, S. Preibisch, C. Rueden, S. Saalfeld, B. Schmid, et al. 2012. Fiji: an open-source platform for biological-image analysis. *Nat. Methods.* 9:676–682. https://doi.org/10.1038/nmeth.2019

Schindelin, J., C.T. Rueden, M.C. Hiner, and K.W. Eliceiri. 2015. The ImageJ ecosystem: an open platform for biomedical image analysis. *Mol. Reprod. Dev.* 82:518–529. https://doi.org/10.1002/mrd.22489

Seshan, A., A.J. Bardin, and A. Amon. 2002. Control of Lte1 localization by cell polarity determinants and Cdc14. *Curr. Biol.* 12:2098–2110. https://doi.org/10.1016/S0960-9822(02)01388-X

Sheltzer, J.M., and M.D. Rose. 2009. The class V myosin Myo2p is required for Fus2p transport and actin polarization during the yeast mating response. *Mol. Biol. Cell.* 20:2909–2919. https://doi.org/10.1091/mbc.E08-09-0923

Shi, Y., K. Barton, A. De Maria, J.M. Petrash, A. Shiels, and S. Bassnett. 2009. The stratified syncytium of the vertebrate lens. *J. Cell Sci.* 122:1607–1615. https://doi.org/10.1242/jcs.045203

Shinn-Thomas, J.H., and W.A. Mohler. 2011. New insights into the mechanisms and roles of cell-cell fusion. Int. Rev. Cell Mol. Biol. 289:149–209.

Simionescu-Bankston, A., G. Leoni, Y. Wang, P.P. Pham, A. Ramalingam, J.B. DuHadaway, V. Faundez, A. Nusrat, G.C. Prendergast, and G.K. Pavlath. 2013. The N-BAR domain protein, Bin3, regulates Rac1- and Cdc42-dependent processes in myogenesis. *Dev. Biol.* 382:160–171. https://doi.org/10.1016/j.ydbio.2013.07.004

Simon, M.-N., C. De Virgilio, B. Souza, J.R. Pringle, A. Abo, and S.I. Reed. 1995. Role for the Rho-family GTPase Cdc42 in yeast mating-pheromone signal pathway. *Nature.* 376:702–705. https://doi.org/10.1038/376702a0

Smith, J.A., and M.D. Rose. 2016. Kel1p mediates yeast cell fusion through a Fus2p- and Cdc42p-dependent mechanism. *Genetics.* 202:1421–1435. https://doi.org/10.1534/genetics.115.185207

Stein, R.A., J.A. Smith, and M.D. Rose. 2015. An amphiphysin-like domain in Fus2p is required for Rvs161p interaction and cortical localization. *G3 (Bethesda).* 6:337–349.

Suetsugu, S. 2016. Higher-order assemblies of BAR domain proteins for shaping membranes. *Microscopy (Oxf.).* 65:201–210. https://doi.org/10.1093/jmicro/dfw002

Suetsugu, S., S. Kurisu, and T. Takenawa. 2014. Dynamic shaping of cellular membranes by phospholipids and membrane-deforming proteins. *Physiol. Rev.* 94:1219–1248. https://doi.org/10.1152/physrev.00040.2013

Trueheart, J., and G.R. Fink. 1989. The yeast cell fusion protein FUS1 is O-glycosylated and spans the plasma membrane. *Proc. Natl. Acad. Sci. USA.* 86:9916–9920. https://doi.org/10.1073/pnas.86.24.9916

Trueheart, J., J.D. Boeke, and G.R. Fink. 1987. Two genes required for cell fusion during yeast conjugation: evidence for a pheromone-induced surface protein. *Mol. Cell. Biol.* 7:2316–2328. https://doi.org/10.1128/MCB.7.7.2316

Vasyutina, E., B. Martarelli, C. Brakebusch, H. Wende, and C. Birchmeier. 2009. The small G-proteins Rac1 and Cdc42 are essential for myoblast fusion in the mouse. *Proc. Natl. Acad. Sci. USA.* 106:8935–8940. https://doi.org/10.1073/pnas.0902501106

Ydenberg, C.A., and M.D. Rose. 2008. Yeast mating: a model system for studying cell and nuclear fusion. *Methods Mol. Biol.* 475:3–20.

Ydenberg, C.A., and M.D. Rose. 2009. Antagonistic regulation of Fus2p nuclear localization by pheromone signaling and the cell cycle. *J. Cell Biol.* 184:409–422. https://doi.org/10.1083/jcb.200809066

Ydenberg, C.A., R.A. Stein, and M.D. Rose. 2012. Cdc42p and Fus2p act together late in yeast cell fusion. *Mol. Biol. Cell.* 23:1208–1218. https://doi.org/10.1091/mbc.E11-08-0723

Zhao, Z.S., T. Leung, E. Manser, and L. Lim. 1995. Pheromone signalling in *Saccharomyces cerevisiae* requires the small GTP-binding protein Cdc42p and its activator CDC24. *Mol. Cell. Biol.* 15:5246–5257. https://doi.org/10.1128/MCB.15.10.5246

Ziman, M., D. Preuss, J. Mulholland, J.M. O'Brien, D. Botstein, and D.I. Johnson. 1993. Subcellular localization of Cdc42p, a *Saccharomyces cerevisiae* GTP-binding protein involved in the control of cell polarity. *Mol. Biol. Cell.* 4:1307–1316. https://doi.org/10.1091/mbc.4.12.1307

Zimmerberg, J., and M.M. Kozlov. 2006. How proteins produce cellular membrane curvature. *Nat. Rev. Mol. Cell Biol.* 7:9–19. https://doi.org/10.1038/nrm1784